Journal of
Nanoscience and Nanotechnology
Vol. 13, 5053–5060, 2013

Catalytic Activity and Structure Properties of Doped $VOHPO_4 \cdot 0.5H_2O$ with Nanosized Ru, Au, Fe and Mn in Benzene Hydroxylation

Peter R. Makgwane[1, 2, *] and Suprakas Sinha Ray[1, 2, *]

[1] *Department of Applied Chemistry, University of Johannesburg, Doornfontein, 2028, South Africa*
[2] *DST/CSIR National Center for Nano-Structured Materials (NCNSM), Council for Scientific and Industrial Research (CSIR), Pretoria, 0001, South Africa*

The promotional effect of nanosized Ru, Fe, Au, and Mn particles on $VOHPO_4 \cdot 0.5H_2O$ (VHP) catalytic properties was investigated in benzene hydroxylation reaction using hydrogen hydroperoxide (H_2O_2) as oxidant. Catalytic results indicated a profound effect of the nanoparticle dopants on VHP catalyst activity and products distribution. Amongst the promoted VHP catalysts, Au/VHP exhibited high catalytic effect with benzene conversion of 76% at a combined 85.5% selectivity toward the formation of phenol and hydroquinone achieved in 6 h under optimised reaction conditions. The extended scope application of nanosized doped Au-VHP showed to provide an effective catalyst for activation of the aromatic hydrocarbons C—H bonds into oxygenate derivatives. The catalyst could be re-used for several cycles with insignificant loss of activity. The doped nanosized Au-VHP catalyst provide a clean promising catalytic route based on heterogeneous catalysis for transformation of aromatics into value-added oxygenates.

Keywords: Vanadium Phosphorus Oxide, Nanosized Particles, Dopants, Oxidation, Hydroxylation, Benzene, Phenol.

RESEARCH ARTICLE

1. INTRODUCTION

Liquid-phase oxidations are important industrial reactions for the functionalization of hydrocarbons into oxygenated chemical derivatives.[1–2] One of such reactions is the hydroxylation of benzene, which yield phenol and its overoxidation products hydroquinone, catechol and benzoquinone that are used as intermediates in the production of other value-added chemicals.[3, 4] The high volume of waste effluents generated by the traditional oxidation processes using strong mineral acids as catalysts is an area of main concern for environmental impact. On the other hand, the increasing pressure from the stringent environmental law requirements imposed on chemical industries continues to be the driving force in the development of green and sustainable catalytic processes.[5] In line of these concerns, the development of effective catalytic oxidation systems that can use the environmentally benign hydrogen peroxide (H_2O_2) oxidants are particularly desirable. The advantages of H_2O_2 as green atom-efficient oxidant is that it yield only water as by-products.

Commercially, phenol is produced by the non-catalysed cumene liquid-phase oxidation or the Hock process.[6] Typically, the cumene oxidation process is performed in a series of cascaded bubble-column reactors operated at 5–10 bar and 100–130 °C in the presence of an aqueous basic Na_2CO_3.[7] The cumene conversion to the cumene hydroperoxide (CHP) content is limited to 30–35% in order to ensure low formation of by-products such as dimethylphenylcarbinol and acetophenone.[6] The obtained CHP is concentrated to about 65–90% in vacuum columns to remove the unreacted cumene which is recycled back to the reactor, while the obtained CHP is acid-cleavaged to phenol and acetone usually by 0.1–2% H_2SO_4 at 60–65 °C.[7] The Hock process constitute several reaction stages that include, (1) preparation of cumene from isopropylation of benzene, (2) oxidation of cumene to CHP, and (3) acid cleavage of CHP into phenol and acetone. This poses serious demands on process economics. On the other hand, the use of mineral acids such as H_2SO_4 usually yield harzadous waste metal salts that are difficult to dispose. Based on the recent demands from the green chemistry chemical conversions protocols, the development of improved catalytic processes that especially use

*Authors to whom correspondence should be addressed.

heterogeneous catalytic route to avoid the use of waste salt generating substrates such as Na_2CO_3 and H_2SO_4 are needed.[5] Consequently, there has been a considerable research interest devoted on realising efficient green catalytic systems for the direct synthesis of phenol from readily available starting materials such benzene without modification or functionalization. Accordingly, the liquid-phase hydroxylation of benzene over several studied solid catalyst using H_2O_2 presents a promising green synthetic protocol to phenol and its derivative chemicals.[3, 4, 8–12]

Vanadium phosphorous oxides (VPOs) on the other hand present highly active catalyst systems with easily changeable V^{4+}/V^{5+} redox properties that give them superior catalytic properties ideal for the activation of C—H and OH bonds into alcohols, ketones, carboxylic acids, etc.[13–15] The enhanced VPOs activity stems from the excellent vanadium metal redox properties and the acidic nature due to intercalated phosphorous element in the catalyst structure. With recent attention directed towards the development of green chemical processing technologies, the VPOs derived catalysts present the desired catalytic properties such as redox and medium acidic nature that are amenable to perform oxidations reactions of hydrocarbons into oxygenates based on their earlier successful application.[16–18] Amongst the VPOs catalyst phases, the studies on catalytic performance of vanadyl hydrogen phosphate hemihydrate, $VOHPO_4 \cdot 0.5H_2O$ (VHP) catalyst phase in liquid-phase oxidations are few.[19, 20] It has been recently reported that VHP catalyst phase is catalytically active as its calcined phase, $(VO)_2P_2O_7$ in the liquid-phase oxidations of aromatic hydrocarbons into oxygenates.[21, 22] Moreover, several groups demonstrated that the activity and selectivity of VPOs catalyst systems can be tailored by the dopants promotional effect.[23–25] Since the excellent vanadium based catalysts catalytic activity is mainly due to the balanced $V^{+3}/V^{+4}/V^{+5}$ redox properties, it can be anticipated that the addition of small amount of metal nanoparticle would influence this oxidation states ratios, thus overall catalytic performance of the catalysts. This can be especially interesting considering the unique structural properties offered by metal catalyst nanoparticles of < 10 nm size with properties that are inaccessible in their bulk form.[26] With that in mind, we are in the present contribution reporting on the catalytic activity of ($VOHPO_4 \cdot 0.5H_2O$) or VHP catalyst doped with nanosized particles of ruthenium (Ru), manganese (Mn), gold (Au) and iron (Fe) metals to improve on catalytic properties of the $VOHPO_4 \cdot 0.5H_2O$ catalyst for hydroxylation reaction of benzene into phenol and its derived products. The enhaced catalytic activity of Ru, Au, Mn and Fe nanoparticles in oxidation reactions have been reported previously in organic synthesis.[27, 28] We show that the combined effect of excellent VHP redox properties and nanosized metal dopants structural properties effect provide a highly reactive VHP catalyst system with efficient conversion rates and satisfying selectivity in the hydroxylation reaction process of benzene and extended scope of application to other aromatics.

2. EXPERIMENTAL DETAILS

2.1. Preparation of Different $VOHPO_4 \cdot 0.5H_2O$ Based Catalysts

The $VOHPO_4 \cdot 0.5H_2O$ (VHP) catalyst was prepared by refluxing V_2O_5 (12.0 g, Aldrich, 99%) and *o*-H_3PO_4 (116 g, 85% Aldrich) in deionised water (300 mL) for 8 h. After the reaction, the yellow $VOPO_4 \cdot 2H_2O$ solid was recovered by vacuum filtration, washed with cold water (100 mL) and acetone (100 mL) and dried in air (110 °C, 12 h). 4 g of $VOPO_4 \cdot 2H_2O$ was refluxed with isobutanol (80 mL) for 21 h, and the resulting blue $VOHPO_4 \cdot 0.5H_2O$ solid was recovered by filtration, refluxed further at 100 °C in deionised water (9 mL H_2O/g solid) for 2 h to remove $VO(H_2PO_4)_2$ impurity phase,[29] filtered hot, and dried in air (110 °C, 16 h).

The promoted VHP nano-catalysts were prepared using $RuCl_3 \cdot xH_2O$, 99.98%; $HAuCl_4 \cdot 3H_2O$, 51.0%; Fe(III) $\cdot 9H_2O$, 99.98%; and $Mn_4 \cdot 3H_2O$, 51.0% metal precursors all from Sigma-Aldrich Chemicals. Initially, promoters nanoparticles were prepared before deposition onto VHP catalyst. The polyvinyl alcohol (PVA) (Aldrich, MW $\sim$ 10000, 80% hydrolysed) was used as a protecting agent. In a typical preparation, the 2 ml of aqueous PVA (2 wt.%) was added to 300 ml of deionised H_2O and the amount of respective promoter was adjusted based on the total w/w% of VHP to be added. The resulting promoter solution was stirred vigorously at 50 °C for 1 h and followed by a rapid injection of few drops ($\sim$ 2 mL) of 0.5 M aqueous $NaBH_4$ (Aldrich Chemicals, 97% purity). The solution was allowed to age for 24 h at room temperature under continuous stirring, thereafter the deposition of VHP was then added under stirring and kept in contact with promoters for 8 h. The nominal amount of respective promoter metals was kept constant at 2 wt.%. The solids were collected by filtration, washed thoroughly with distilled water and acetone, respectively, and dried in an air oven at 120 °C for 24 h. The catalysts so-prepared were denoted as Au/VHP, Ru/VHP, Fe/VHP, and Mn/VHP, respectively.

2.2. Characterisation Procedures of Catalyst

Total specific surface area and pore volume of VHP based catalysts were measured by nitrogen physisorption at 77 K, using a Micromeritics TRISTAR 3000 instrument. Before N_2 physisorption, the samples were degassed at 120 °C for 12 h under a continuous flow of N_2 gas to remove adsorbed contaminants. The spectra were recorded with a resolution of 2 cm^{-1}. X-ray diffraction (XRD) experiments were recorded on a PAnalytical XPERT-PRO diffractometer measurement, using Ni filtered CuKα radiation ($\lambda =$ 1.5406 Å) at 40 kV/50 mA. The diffraction measurements

RESEARCH ARTICLE

were collected at room temperature in a Bragg-Brentano geometry with scan range, $2\theta = 10$–$70°$ using continuous scanning at a rate of 0.02 °/s. The nanoparticles dimensions of the catalysts were measured by High Resolution-Transmission Electron Microscopy (HR-TEM) JEOL JEM 2100, operated at an accelerating voltage of 200 kV. Before TEM analysis, the samples were prepared by suspending the solid in ethanol and submitting the suspension to ultrasonication for 30 min. Afterward a drop was extracted placed on holly carbon-coated copper grid for TEM measurements. The Raman spectra were recorded with a T64000 Raman spectrometer from HORIBA Scientific, Jobin Yvon Technology (Villeneuve d'Ascq, France). The Raman spectra were excited with either the 514.5 nm lines of a Coherent Innova® 70C Series Ion Laser System and the 100× or 50× objectives of an Olympus microscope was used to focus the laser beam (spot size ~2–12 μm) on the samples and also collected the backscattered Raman signal. An integrated triple spectrometer was used in the double subtractive mode to reject Rayleigh scattering and dispersed the light onto a liquid nitrogen-cooled Symphony CCD detector.

2.3. Catalytic Activity Testing Procedure

The catalytic activity testing was done in a 50 ml two necked round bottom flask equipped with the magnetic stirrer and reflux condenser. The reactor was charged with benzene (10 mmol), 50% H_2O_2 (30 mmol) catalyst (0.10 g) and 6 mL acetonitrile (CH_3CN) solvent. The temperature of the reaction was controlled by immersing the reactor in an oil bath. Samples withdrawn from the reactor containing the benzene oxidation products were analyzed using a Supelco SPB-20 column (30 m × 0.25 mm i.d. × 0.25 mm) on Agilent 7890A Gas Chromatograph (GC) equipped with flame ionization detector (FID). GC analysis program was as follow: FID temperature (300 °C), injector temperature (250 °C), and oven column temperature, 80 °C (3 min) then ramped to 220 °C at 10 °C/min and split was 1:100 at constant flow rate. To study the possible metal catalyst leaching, we used the following reaction conditions (catalyst = 0.1 g, temperature = 70 °C and time = 1 h). After the 1 h reaction time, the catalyst was separated by filtration while the reaction liquid mixture was hot and the reaction was allowed to react further for a total reaction time of 3 h. For catalyst recyclability testing experiments, after each reaction cycle the catalyst was filtered from the liquid solution and washed with acetone followed by drying in the air for 2 h at 110 °C before use in the next cycle.

3. RESULTS AND DISCUSSION

3.1. Catalytic Activity Measurements

Initially, in the catalytic activity testing of different promoted VHP and pure VHP catalysts, we first performed the blank reaction of benzene and H_2O_2 oxidant in the absence of catalyst in order to establish the base performance of the non-catalytic reaction. The reaction gave only less than 1% benzene conversion after 3 h (Table I). This indicated that the free radicals chain-initiation rates are slow in the absence of the catalyst irrespective of the added reactive H_2O_2 oxidant. When the same reaction was performed with pure VHP and different metal nanoparticles doped-VHP catalysts, there was a substantial increase of conversion from less than 1% in the non-catalysed reaction to 14% or more indicating the significant catalytic effect under similar reaction conditions (Table I). This demonstrated the active participation of VHP catalyst in the activation of benzene C—H bond via homolytic catalytic cleavage of O—O bond of H_2O_2 into highly reactive free radicals capable to initiate the chain oxidation mechanism. Moreover, the slow chain initiation rates for the non-catalysed reaction are in agreement with the reported findings, that self-thermal decomposition of H_2O_2 into reactive oxygen radicals species to initiate the hydrocarbons oxidations chain reactions is inadequate.[30] The catalytic decomposition of HOOH by vanadium is assumed to occur via the formation of either coordinated vanadium hydroperoxo species or vanadium peroxo species that are oxygen-donors to facilitates the transfer of electrophilic oxygen to the formed free radicals.[2]

Table I. Catalytic activity performance of different VHP based catalysts in benzene hydroxylation.

		Selectivity (%)			
Catalyst	Benzene conversion (%)	Phenol	[a]HQ	Others	Phenol/HQ
Blank	< 1	100.0	–	–	
VHP	14.2	55.3	16.6	28.1	71.9
Fe/VHP	22.6	59.2	23.9	16.9	83.1
Mn/VHP	18.8	51.3	18.7	30.0	70.0
Au/VHP	48.3	65.2	23.3	11.5	88.5
Ru/VHP	32.8	70.2	21.6	8.2	91.8

Notes: Reaction conditions: benzene (10 mmol) and 50% H_2O_2 (30 mmol), 0.10 g catalyst, CH_3CN (6 ml), $T = 70$ °C and $t = 3$ h. [a]HQ = hydroquinone.

The effect of nanosized Au, Ru, Mn, and Fe particles dopants on VHP catalyst performance was significantly pronounced on both activity and products distribution pattern. For example, Au and Ru as VHP dopants gave better activities with conversions in a range of 32–50%, which were higher than the one achieved with the pure VHP catalyst of 14.2%. On the other hand, the Mn/VHP and Fe/VHP catalysts performance was poor showing low conversions of 18.8.5% and 22.6%, respectively. In addition to the low catalytic activity displayed by Mn/VHP, the catalyst also showed poorly combined selectivity towards phenol and hydroquinone formation of 70.0% compared to Au/VHP of 88.5%. However, Ru/VHP catalyst showed slightly high phenol/hydroquinone selectivity of 91.8% although its conversion was lower than the one obtained with Au/VHP catalyst. The low benzene conversion and

Table II. Effect H_2O_2 concentration on benzene hydroxylation rates using doped-Au/VHP catalyst.

Benzene/H_2O_2 molar ratio	Benzene conversion (%)	Selectivity (%)			
		Phenol	HQ	Others	Phenol/HQ
1	14.3	83.2	10.6	6.2	94.8
2	36.8	73.5	18.3	8.2	91.8
3	48.3	72.8	15.7	11.5	88.5
4	53.6	62.4	12.4	25.2	74.8
5	56.8	61.4	10.6	28.0	72.0

Notes: Reaction conditions: benzene (10 mmol), Au/VHP catalyst (0.10 g), CH_3CN (6 ml), $T = 70$ °C and $t = 3$ h. HQ = hydroquinone.

poor products selectivity toward phenol/hydroquinone displayed by the Mn/VHP and Fe/VHP catalysts can be attributed to the possible coverage of VHP catalyst active sites probably due to the formation of large particles size and particles clustering as confirmed later by TEM results (Fig. 5).

Based on the catalytic activity results obtained for different promoted VHP catalysts and their product selectivity (Table I), the nanosized doped-Au/VHP was chosen as the best performing catalyst to further investigate the effect of other reaction parameters on the oxidation rates. The effect of the molar ratio of benzene and H_2O_2 oxidant on hydroxylation rates and products selectivity was studied in a range of 1:1 to 1:5 using Au/VHP nanosized-doped catalyst. The results obtained are listed in Table II. The conversion of benzene increased significantly with the increasing H_2O_2 oxidant molar ratio to benzene from 14.3% at 1:1 to 48.3% at 1:3 and thereafter started to show raising slowly up to 56.8%. On the other hand, the selectivity towards combined phenol/Hydroquinone dropped relatively from 94.8% at 1:1 molar ratio to 72.0% at 1:5. The overoxidation of benzene into other products apart from the phenol and hydroquinone formation was observed to be serve at higher H_2O_2 concentrations above 1:3 ration with respect benzene. Consequently, the 1:3 ratio seems to give the acceptable conversion rates of 48.3% at the preserved combined selectivity of 88.5% toward the formation of phenol and hydroquinone.

Figure 1 illustrates the time-dependence evolution of benzene conversion rate and different products selectivity using the nanosized doped-Au/VHP catalyst. The conversion rate of benzene increased gradually up to about 62% conversion at 4 h, and then thereafter started to show reaching the plateau with the increasing reaction time to the maximum conversion of up to 76% after 8 h. At 76% benzene conversion, phenol and hydroquinone were the major products with respective selectivities of 61% and 24.5% or combined of 85.5%.

To evaluate the stability of the catalyst activity with time on-stream, the nanosized doped-Au/VHP catalyst was reused for five consecutive batch oxidation cycles (Fig. 2). Each reaction cycle was performed under similar reaction conditions for 8 h. After each reaction cycle, the used

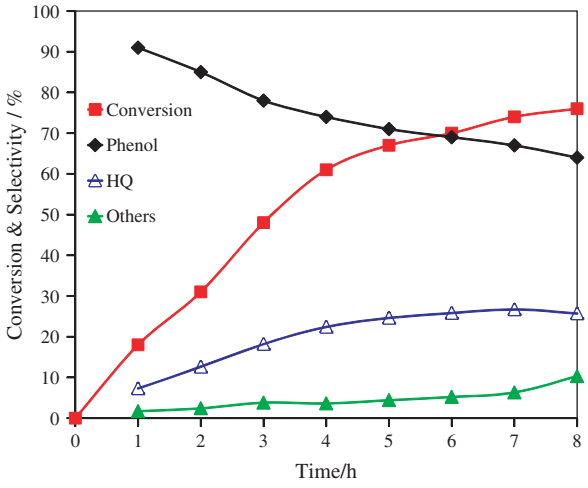

Fig. 1. Time-courses dependence of benzene conversion and products selectivity using nanosized doped-Au/VHP catalyst. Reaction conditions: benzene (10 mmol), 50% H_2O_2 (30 mmol), catalyst (0.10 g), CH_3CN (6 ml), $T = 70$ °C.

catalyst was separated by filtration followed by washing with acetone and drying in an oven for 2 h at 110 °C before use in the next reaction cycle. Although it was difficult to recover the catalyst in the lab-scale due to a small amount of few milligrams usually used, we maintained the catalyst recovery of 93–96% based on the initial mass used for each reaction cycle. The catalyst did not show any significant change in activity after 5 reuse testing cycles with the benzene conversion stabilized at around 73–77%. Inversely, the selectivity of phenol changed slightly in a range of 63–66%. The short window period recyclability testing of nanosized doped-Au/VHP catalyst in the present study give only the rough estimation of its performance but not the true long-term performance deactivation that usually requires several hundred hours of on-stream testing.[22] This would require the use of a well-controlled reactor such as continuous-flow system (e.g., micro-channels or fixed-bed reactor) that will ensure uniform contact of reactants with the catalyst material for a prolonged usage period without the significant limitations imposed by the loss of the catalyst mass.

Based on the succesfull application of nanosized doped-Au/VHP as effective hydroxylation catalyst for benzene reaction to phenol, we expanded the catalyst scope of application to other industrially important aromatics and cyclic ring hydrocarbons such as toluene, styrene and cyclohexane under the similar optimized reaction conditions. The toluene hydroxylation is an important reaction route for the synthesis of benzyl alcohol, benzaldehyde, benzoic acid and cresols,[31] while styrene hydroxylation leads to the formation of flavor and fragrance intermediate, benzaldehyde isolated in high yields.[32] Similarly, the hydroxylation of cyclohexane is an industrially important reaction process for the synthesis of cyclohexanol and cyclohexanone as intermediates to adipic acid for the production of nylon

Table III. Scope application of nanosized doped-Au/VHP in hydroxylation of different aromatics.

Entry	Substrate	Conversion (%)	Selectivity to major products (%)			
1		71.0	Phenol (61.0)	Hydroquinone (24.5)	–	–
2		68.3	Cyclohexanol (58.4)	Cyclohexanone (25.8)	–	–
3	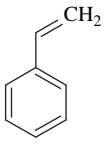	73.7	Benzaldehyde (48.0)	Benzyl alcohol (10.2)	Benzoic acid (23.6)	–
4	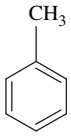	36.0	Benzaldehyde (60.1)	Benzyl alcohol (12.7)	Benzoic (9.2)	Cresols (10.8)

Note: Reaction conditions: benzene (10 mmol) and 50% H_2O_2 (30 mmol), 0.10 g catalyst, CH_3CN (6 ml), $T = 70$ °C and $t = 8$ h.

relater polymer products.[33] It can be seen in Table III that the nanosized doped-Au/VHP catalyst showed catalytic effect in all tested hydroxylation reactions giving efficient substrates conversions. Interestingly, was the high catalytic activity displayed by nanosized doped-Au/VHP on cyclohexane oxidation with much improved substrate conversion at preserved high selectivity toward the formation cyclohexanol and cyclohexanone products. Commercially, the cyclohexane oxidation process is limited to 5–10% conversion in order to preserve selectivity which is in a range of 85–90%. By comparison, our present catalysed cyclohexane liquid-phase oxidation reaction performed better than that of the industrial cyclohexane oxidation process. A cyclohexane conversion of 68.3% at cyclohexanol and cyclohexanone combined selectity of 84.2% was achieved using the nanosized doped Au-VHP catalyst. The results obtained for nanosized doped-Au/VHP catalyst in Table III present a facile catalytic synthetic protocol of converting various aromatics or cyclic ring hydrocarbons into functionalized oxygenates of industrial importance that can be extended to other typical reactions.

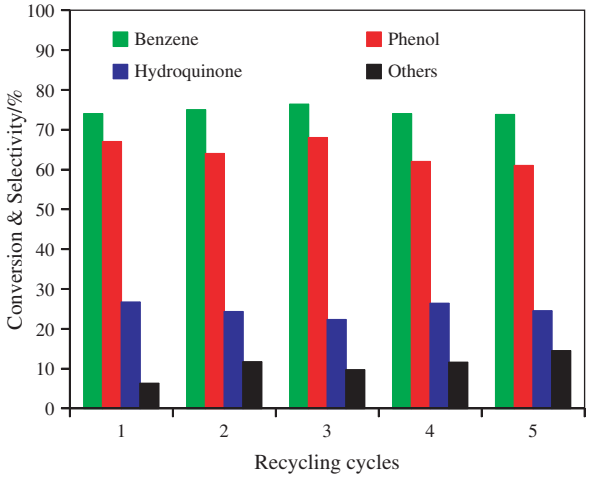

Fig. 2. Recyclability testing of nanosized doped-Au/VHP catalyst in benzene hydroxylation reaction. Reaction conditions: benzene (10 mmol), 50% H_2O_2 (30 mmol), catalyst (0.10 g), CH_3CN (6 ml), $T = 70$ °C, $t = 8$ h.

3.2. Characterisation of Catalyst Materials

To understand the correlation between the structure properties of the different nanosized particle doped-VHP catalysts and their catalytic performance in benzene liquid-phase oxidation, the catalysts were characterized using XRD, HR-TEM, Raman and N_2 physisorption. The XRD structural patterns of the pure and promoted VHP catalysts are presented in Figure 3. The results confirmed the formation of the XRD diffraction patterns assignable to the VHP catalyst phase (PDF file JCP2 00-047-0953) (Fig. 3). For different promoted VHP catalysts, there were detectable presence of XRD peaks assigned to some of the promoter metals, otherwise others showed mainly VHP diffraction patterns. For example, the broader peaks of metallic Au nanocatalyst at $2\theta = 38°$ and 44° are visible in the XRD patterns, Figure 3 marked with Au.[34] The diffraction peak of RuO_2 nanocrystalline that usually appear at $2\theta = 35°$ could not be observed. This is probably due to either well-dispersion or low loading of RuO_2 (2 wt.%). Similarly, for Fe/VHP and Mn/VHP promoted catalysts it was difficult to recognise XRD diffraction peaks assignable to them. The XRD peaks of Mn phases of MnO and MnO_2 usually

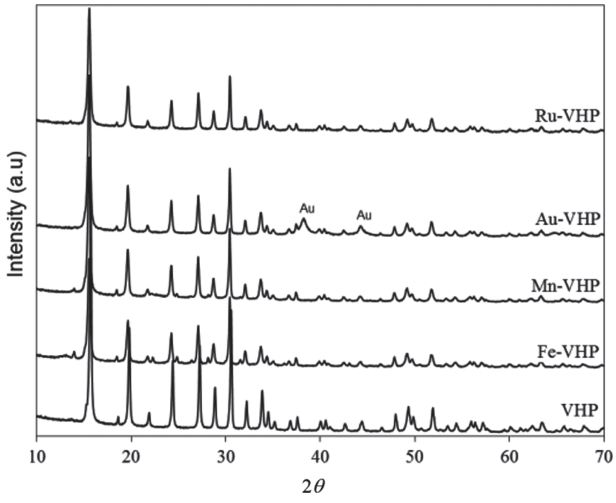

Fig. 3. XRD patterns of pure VHP and different nanosized doped-VHP catalysts.

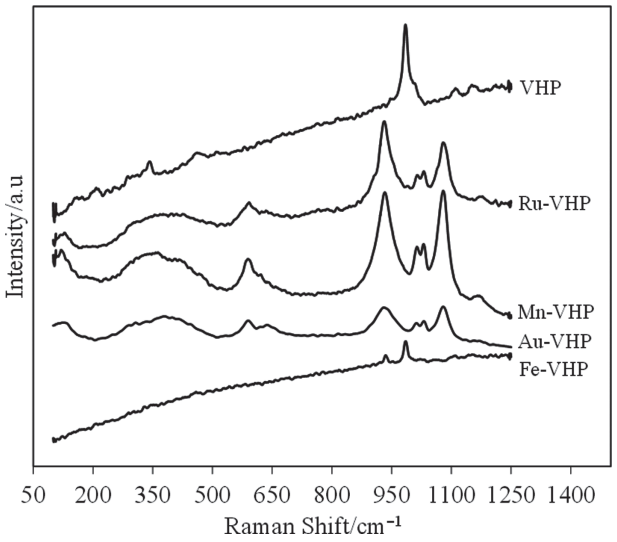

Fig. 4. Raman analysis of pure VHP and different nanosized doped-VHP catalysts.

appear at approximately, $2\theta = 31°$, 41° and 48° lines but these lines seems to be overlapping with the diffraction patterns of the VHP catalyst. Nevertheless, the presence of the different metals on the VHP surface although some were not detectable by the XRD analysis was confirmed by the EDX mesurements (Table IV) and TEM images (Fig. 5).

Figure 4 illustrates the Raman analysis of different VHP based catalysts. The pure VHP showed similar Raman bands to the literature reported $VOHPO_4 \cdot 0.5H_2O$ structure dominated by an intense band at 985.76 cm^{-1}.[37] The band at 982 cm^{-1} had been assigned to V—O—P vibrational mode while the additional two minor bands appearing at 1110 and 1151 cm^{-1} belongs to the P—O stretching bonds of the VHP.[35] Other low intense bands assignable to VHP are noticeable at lower Raman region of 200–600 cm^{-1}. Some of these bands are also visible in the doped-VHP catalyst with different nanosized metal particles. The Ru/VHP, Au/VHP and Mn/VHP catalyst also showed the formation of new intense band at around 600 cm^{-1} that was not observed in the pure VHP and Fe/VHP doped catalysts Raman bands. The peak belonging to VHP (982 cm^{-1}) was more visible in the Fe/VHP doped catalysts, while other doped indicated possible shift or covered by the additional two high intense peaks appearing at 926 and 1076 cm^{-1} for Ru/AHP, Au/VHP and Mn/VHP catalysts are related to the PVA.[36] These different structural phases or bands for nanosized metal doped-VHP enunciate the possible structural difference of VHP induced by the nature of the promoter metals which can have significant influence on their catalytic activity as observed in Table I.

Table IV. Physico-chemical properties of promoted VHP catalysts.

Catalyst	[a]Loadings (wt.%)	Surface area (m^2/g)	Pore volume (cm^3/g)
VHP	–	14.3	0.23
Ru/VHP	1.25	19.3	0.17
Au/VHP	1.18	15.1	0.19
Mn/VHP	1.36	9.6	0.22
Fe/VHP	1.09	13.4	0.20

Note: [a]Measured by EDX.

Figure 5 illustrates the TEM images of different promoted VHP catalysts, including the reference pure VHP catalyst phase. The TEM images of all promoted VHP catalysts showed plate-like layers structural morphology typical of vandium phosphorous oxide catalyst systems (Figs. 5(a)–(d)).[29] These platelets layers showed a stacked together arrangement on top of each other with the average mean particles size in a range of 30–50 nm as illustrated for the pure VHP catalyst in Figure 5(e). For both nanosized doped-Au/VHP and Ru/VHP catalysts, they showed the formation of well-dispersed particles with a mean size in the range of 5–9 nm which could be related to their better observed catalytic activity in table. The Fe/VHP catalyst indicated possible particles aggregates clusters although it showed the formation of small nanosize particles comparable to those of Ru/VHP and Au/VHP doped catalysts (Fig. 5(d)). Inversely, the Mn/VHP catalyst indicated the formation of large clustered particles with size greater than 10 nm or equivalent to the VHP platelets in some instances (Fig. 5(b)). The large particles size formation of Mn on VHP, thus showing to be covering its surface can be assumed to be responsible for the poor catalytic activity performance observed Mn/VHP catalyst in Table I.

The textural and physical data of the pure and doped VHP catalysts are summarised in Table IV. The BET surface areas of the pure VHP catalyst was found to be 13 m^2/g while VHP doped with nanosize particles of

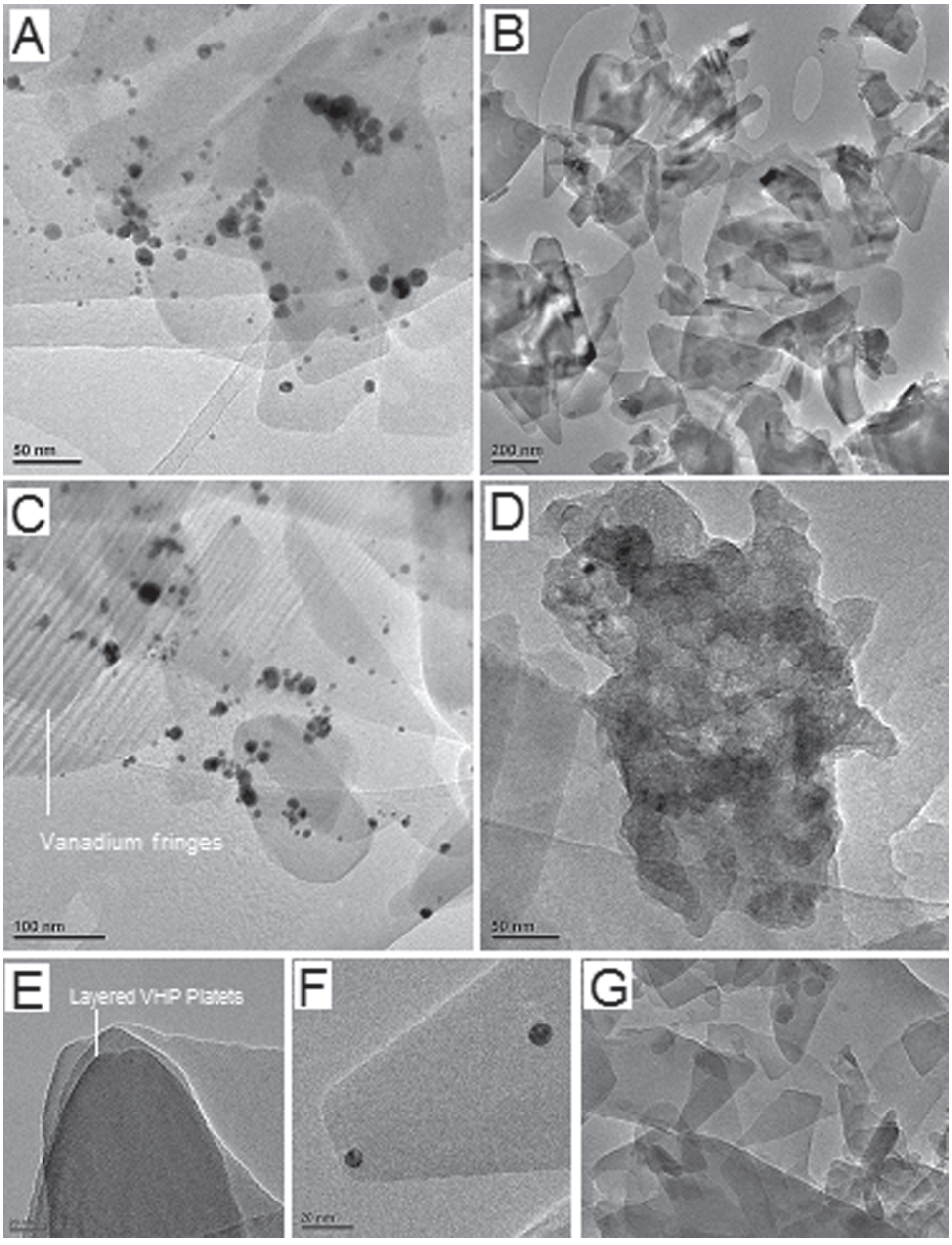

Fig. 5. TEM images of different nanosized doped-VHP based catalysts. (a) Au/VHP, (b) Mn/VHP, (c) Ru/VHP, (d) Fe/VHP, (e) layered platelets of pure VHP, (f) nanoparticles of Ru on VHP single layer and (g) overlapping VHP platelets with visible dark-spot nanoparticles in-between the platelets layers.

different metals showed varying surface areas depending on the nature of the dopant. The Ru, Fe, and Au doped VHP catalysts showed slightly higher surface areas than the pure VHP catalyst. Such an observation may be due to small nanosize particles as indicated by TEM results. On the other hand, the Mn/VHP promoted catalyst displayed a drop in surface area, which could be attributed to Mn large particles size formation on the surface or interacting with VHP (Fig. 5). Similarly, the pore volume of the promoted VHP catalysts indicated no noticeable variation with a significant trend. These structural differences can have a profound effect on VHP catalytic performance as observed in Table I, probably due to electronic effect on V^{+4}/V^{+5} ratio of the synthesized VHP catalysts.

4. CONCLUSION

In summary, the catalytic results obtained showed that the catalytic properties of VHP catalyst in the hydroxylation reaction of benzene using H_2O_2 as oxidant can enhanced siginificantly by the used of nanosized metal particles effect. The most interesting observation was that the catalysts were highly active without being calcined or activated as usually done for VPO catalyst system. Amongst

the doped-VHP catalysts, Ru/VHP exhibited excellent catalytic performance and reusability after several consecutive testing. A benzene conversion of up to 76% at 85.5% total selectivity towards the formation of phenol and hydroquinone was obtained using nanaosized doped Au-VHP catalyst. Inversely, the Mn/VHP catalyst exhibited low activity that indicated that the Mn promotion inhibited the catalytic active sites of VHP catalyst. Based on characterisation results, the influence induced by the different promoter metals electronic and structural properties are proposed to be of importance to improve the VHP catalyst catalytic performance probably related to the enhanced V^{+5}/V^{+4} ratio. Moreover, the most significant finding with the different promoted VHP catalysts was that, the metal dopants in their nanosized particle forms allow improving the VHP catalytic properties. The catalytic activity displayed by doped-$VOHPO_4 \cdot 0.5H_2O$ provide efficient catalytic routes for conversion of several studied aromatics into intermediates of important industrial application.

Acknowledgments: Authors are grateful for the financial support from the University of Johannesburg and the National Research Foundation (NRF) of South Africa. The DST/CSIR National Centre for Nano-Structured Materials is thanked for providing with research equipment to perform this work. Dr. Linda Prinsloo (University of Pretoria) is thanked for helping Raman analysis.

RESEARCH ARTICLE

References and Notes

1. A. K. Suresh, M. M. Sharma, and T. Sridhar, *Ind. Eng. Chem. Res*. 39, 3958 **(2000)**.
2. R. A. Sheldon and J. K. Kochi, Metal-Catalyzed Oxidation of Organic Compounds, Academic Press, New York **(1981)**.
3. X. Qi, J. Li, T. Ji, Y. Wang, L. Feng, Y. Zhu, X. Fan, and C. Zhang, *Microporous and Mesoporous Materials* 122, 36 **(2009)**.
4. S. Song, H. Yang, R. Rao, H. Liu, and A. Zhang, *Catal. Commun*. 11, 783 **(2010)**.
5. R. A. Sheldon, *Chem. Soc. Rev*. 41, 1437 **(2012)**.
6. R. J. Schmidt, *Appl. Catal. A: Gen*. 280, 89 **(2005)**.
7. V. M. Zakoshansky, K. Griaznov, I. L. Vasilieva, J. W. Fulmer, and W. D. Kight, Cumene oxidation process, US Patent 5.767,322 **(1988)**.
8. Y. Leng, H. Ge, C. Zhou, and J. Wang, *Chem. Eng. J*. 145, 335 **(2008)**.
9. C. A. Antonyraj and S. Kannan, *Appl. Clay Sci*. 53, 297 **(2011)**.
10. D. Barbera, F. Cavani, T. D'Alessandro, G. Fornasari, S. Guidetti, A. Aloise, G. Giordano, M. Piumetti, B. Bonelli, and C. Zanzottera, *J. Catal.* 275, 158 **(2010)**.
11. Y.-Y. Gu, X.-H. Zhao, G.-R. Zhang, H.-M. Ding, and Y.-K. Shan, *Appl. Catal. A: Gen*. 328, 150 **(2007)**.
12. S. Song, H. Yang, R. Rao, H. Liu, and A. Zhang, *Appl. Catal. A: Gen*. 375, 265 **(2010)**.
13. G. Centi and F. Trifiró, *Chem. Rev.* 88, 55 **(1988)**.
14. K. Aï-Lachgar, M. Abon, and J. C. Volta, *J. Catal.* 171, 383 **(1997)**.
15. E. Mikolajska, E. R. Garcia, R. López-Medina, A. E. Lewandowska, J. L. G. Fierro, and M. A. Bañares, *Appl. Catal. A: Gen.* 404, 93 **(2011)**.
16. G. C. Behera and K. M. Parida, *Appl. Catal. A: Gen*. 413–414, 245 **(2012)**.
17. P. Borah, C. Pendem, and A. Datta, *Stud. Surf. Sci. Catal*. 175, 541 **(2010)**.
18. I. Sádaba, S. Lima, A. A. Valente, and M. López-Granados, *Carbohydr. Res*. 46, 2785 **(2011)**.
19. P. R. Makgwane, E. E. Ferg, D. G. W. Billing, and B. Zeelie, *Catal. Lett*. 135, 105 **(2010)**.
20. U. R. Pillai and E. Sahle-Demessie, *New J. Chem*. 27, 525 **(2003)**.
21. P. R. Makgwane, N. I. Harmse, E. E. Ferg, and B. Zeelie, *Chem. Eng. J*. 162, 341 **(2010)**.
22. P. R. Makgwane, E. E. Ferg, and B. Zeelie, *ChemCatChem* 3, 180 **(2011)**.
23. J. Liu, F. Wang, Z. Gu, and X. Xu, *Chem. Eng. J*. 151, 319 **(2009)**.
24. A. Martin, U. Bentrup, and G.-U. Wolf, *Appl. Catal. A: Gen*. 227, 131 **(2002)**.
25. Y. H. Taufiq-Yap, S. Nor Asrina, G. J. Hutchings, N. F. Dummer, and J. K. Bartley, *J. Natural Gas* 162, 31 **(1996)**.
26. M. Choi, C. Han, I. T. Kim, J. C. An, J. J. Lee, H. K. Lee, and J. Shim, *J. Nanosci. Nanotechnol*. 11, 838 **(2011)**.
27. K. Ki-Joong, S. Jae-Koon, S. Seong-Soo, K. Sang-Jun, C. Min-Chul, J. Sang-Chul, J. Woon-Jo, and A. Ho-Geun, *J. Nanosci. Nanotechnol*. 11, 1605 **(2011)**.
28. S, Bhattacharjee, J. S. Choi, S. T. Yang, S. B. Choi, J. Kim, and W. S. Ahn, *J. Nanosci. Nanotechnol*. 10, 135 **(2010)**.
29. C. J. Kiely, A. Burrows, S. Sajip, G. J. Hutchings, M. T. Sananes, A. Tuel, and J.-C. Volta, *J. Catal.* 162, 31 **(1996)**.
30. I. Hermans, P. A. Jacobs, and J. Peeters, *Chem. Eur. J.* 12, 4229 **(2006)**.
31. J.-L. Li, X. Zhang, and X.-R. Huang, *Phys. Chem. Chem. Phys*. 14, 246 **(2012)**.
32. J. K. Joseph, S. Singhal, S. L. Jain, R. Sivakumaran, B. Kumar, and B. Sain, *Catal. Today* 141, 211 **(2009)**.
33. Z. Sun, G. Li, L. Liu, and H. Liu, *Catal. Commun*. 27, 200 **(2012)**.
34. M. S. Chen and D. W. Goodman, *Catal. Today* 111, 22 **(2006)**.
35. R. Tanner, P. Gill, R. Wells, J. E. Bailie, G. Kelly, S. D. Jackson, and G. J. Hutchings, *Phys. Chem. Chem. Phys.* 2, 688 **(2002)**.
36. C.-C. Yang, Y.-J. Lee, and J. M. Yang, *J. Power Sources* 188, 30 **(2009)**.

Received: 31 October 2012. Accepted: 15 January 2013.